The Human Immunodeficiency Virus gp120 Binding Site on CD4: Delineation by Quantitative Equilibrium and Kinetic Binding Studies of Mutants in Conjunction with a High-Resolution CD4 Atomic Structure

By Ulrich Moebius,[*][‡] Linda K. Clayton,[*][‡] Sheena Abraham,[*] Stephen C. Harrison,[||] and Ellis L. Reinherz[*][§]

From the [*]Laboratory of Immunobiology, Dana Farber Cancer Institute, and the Departments of [‡]Pathology and [§]Medicine, Harvard Medical School, Boston, Massachusetts 02115; and the [||]Department of Biochemistry and Molecular Biology, and Howard Hughes Medical Institute, Harvard University, Cambridge, Massachusetts 02138

Summary

The first immunoglobulin V–like domain of CD4 contains the binding site for human immunodeficiency virus gp120. Guided by the atomic structure of a two-domain CD4 fragment, we have examined gp120 interaction with informative CD4 mutants, both by equilibrium and kinetic analysis. The binding site on CD4 appears to be a surface region of about 900 Å^2 on the C" edge of the domain. It contains an exposed hydrophobic residue, Phe43, on the C" strand and four positively charged residues, Lys29, Lys35, Lys46, and Arg59, on the C, C', C", and D strands, respectively. Replacement of Phe43 with Ala or Ile reduces affinity for gp120 by more than 500-fold; Tyr, Trp, and Leu substitutions have smaller effects. The four positively charged side chains each make significant contributions (7–50-fold). This CD4 site may dock into a conserved hydrophobic pocket bordered by several negatively charged residues in gp120. Class II major histocompatibility complex binding includes the same region on CD4; this overlap needs to be considered in the design of inhibitors of the CD4-gp120 interaction.

The CD4 transmembrane glycoprotein participates in key steps of thymocyte differentiation (1–3) and T lymphocyte activation (4–9) by interacting with nonpolymorphic regions of class II MHC molecules (10–12). It is expressed on most thymocytes (1) and a subset of T lymphocytes, including helper T cells and class II MHC-specific cytotoxic T cells (5–7, 13, 14). CD4 in humans is also the receptor for HIV (15–18). It is required for viral attachment and subsequent entry into cells (19), and these functions account for HIV T cell tropism. The virus binds through a contact made by the gp120 component of its envelope glycoprotein (20). The binding of gp120 to CD4 has been implicated in the cellular depletion of CD4+ lymphocytes in AIDS (21–24), and circulating free gp120 is thought to interfere with normal immune function (12, 25). The central role of the CD4-gp120 interaction in the pathogenesis of AIDS justifies a detailed analysis in molecular terms, and inhibition of that interaction is also an attractive target for antiviral intervention.

The extracellular part of CD4 contains four Ig-like domains (26). The gp120 binding site lies in the most NH$_2$ terminal of these domains (27, 28). A number of studies employing escape mutants (29), insertion mutagenesis (30), homology scanning mutagenesis (12, 28, 31), and alanine scanning mutagenesis (32) have helped to restrict the binding site to a segment surrounding the region homologous to the CDR2 of an Ig V domain.

The atomic structure of a fragment containing the first two domains of CD4 has been determined by x-ray crystallography (33, 34). The first domain contains two antiparallel β sheets, as predicted by its Ig V homology. The mutations that affect gp120 binding lie mostly in the antiparallel strands, denoted C' and C", that form a ridge at one edge of the domain as well as in the adjacent D strand. The C'C" loop is longer than the CDR2 loop of a typical Ig V domain, and it projects prominently from the surface of the molecule (33).

The experiments reported here were designed to obtain quantitative measurements of the contributions made by individual amino acid side chains to gp120 binding. Informed by the atomic structure, we have substituted exposed and buried residues in domain 1 of CD4 and we have analyzed these mutants, in which only local perturbations of structure occur.

The affinity of these mutants for gp120 has been determined at 37°C, where equilibrium can be reached, rather than at the lower temperature used in many previous reports (12, 28, 30–32). We can therefore distinguish effects on the equilibrium binding constant from effects on the association rate constant. We have also measured the kinetics of association and dissociation. Our results show that the key binding surface for gp120 contains an exposed hydrophobic residue with spatially adjacent, positively charged amino acids. The structure of the hydrophobic side chain and the positive charges on the surrounding residues are both important for the gp120 interaction. These features are critical for the interaction with gp120 from different HIV strains, despite substantial sequence differences between them.

Materials and Methods

Antibodies and Cells. CD4 mAbs 19Thy5D7 and 18T3A9 have been described previously (7). RFT4 was provided by Dr. G. Janossy (Royal Free Hospital, London), and BL410T4 and VIT4 were obtained through the Third Leukocyte Typing Workshop. Anti-HIV-I gp120 mAb specific for HIVIIIB gp120 was purchased from New England Nuclear-DuPont (Wilmington, DE). mAb F59.1 reactive with gp120 from strain SF2 was obtained from Repligen (Cambridge, MA). Recombinant gp120 from HIV strains IIIB and SF2 were provided by the AIDS program, National Institute of Allergy and Infectious Diseases, National Institutes of Health (Rockville, MD) and Chiron Inc. (Emeryville, CA), respectively. OKT4 hybridomas cells were obtained from American Type Culture Collection (Rockville, MD). MA5.8 cells were the kind gift of J. Ashwell (NIH). PBL were prepared from whole blood by gradient centrifugation employing Ficoll-Hypaque (Pharmacia Fine Chemicals, Piscataway, NJ). Culture medium was RPMI (Gibco Laboratories, Grand Island, NY) containing 10% FCS (Sigma Chemical Co., St. Louis, MO), 200 mM glutamine (Gibco Laboratories), 100 mM Na-pyruvate (Gibco Laboratories), penicillin/streptomycin (Gibco Laboratories), and 5×10^{-5} M 2-ME (Sigma Chemical Co.).

Site-directed Mutagenesis and Transfection. A transmembrane version of CD4 that has been previously subcloned into M13mp18 (35) was used as template for oligonucleotide-directed mutagenesis using a mutagenesis kit (Amersham Corp., Arlington Heights, IL). Single-stranded DNA was prepared and mutagenesis performed according to the manufacturer's recommendations. Oligonucleotides encoding single amino acid substitutions (18–22 bases) were synthesized using standard cyanoethyl phosphoramodite chemistry. The presence of mutations was confirmed by sequencing M13mp18-CD4 constructs. Mutant CD4 inserts were excised with XbaI and subcloned into the XbaI side of the vector Pink-2 (36). Pink-2-CD4 plasmid DNA was purified using a plasmid kit (Qiagen, Chatsworth, CA) and was sequenced using double-stranded DNA as template in order to confirm each mutation in the expression vector. All mutations were verified by sequencing the DNA encoding domain 1. Mutant T45A contained a second point mutation, I24T. However, since an independent I24T mutation did not affect HIV binding (35), we consider the effect of this mutant to be due to the alteration of residue 45. Mouse T hybridoma cell line MA5.8 (2×10^7 cells) was transfected with 15 µg linearized (XmnI digested) plasmid DNA by electroporation (Cell Porator; 300 V, 1,100 µF; Bethesda Research Laboratories, Gaithersburg, MD). Cells were plated at 3×10^5 cells/ml in culture medium in 24-well plates. At 48 h posttransfection, the medium was replaced with culture medium containing 1 mg/ml G418 (Gibco Laboratories). Growing colonies were transferred, expanded in medium with 0.5 mg/ml G418 and subsequently tested for CD4 expression by immunofluorescence using OKT4.

gp120 Binding. For equilibrium binding assays, 2×10^5 cells in 4-ml tubes and 0.1 ml culture medium containing 0.002% Na-Azide were incubated with different concentrations of gp120 at 37°C in 5% CO_2-humidified atmosphere for 8–12 h. Cells were washed and processed for immunofluorescence. In on-rate experiments cells were incubated as above, but gp120 (about threefold K_d) was added at different time points. All samples were processed together for immunofluorescence. In off-rate experiments, 3×10^6 cells were incubated in 0.5 ml culture medium containing 0.002% Na-Azide and saturating concentrations of gp120 at 37°C for 1 h. Samples were washed twice and incubated at 4°C. Aliquots of 3×10^5 cells (0.1 ml) were transferred to 1 ml prewarmed (37°C, waterbath) medium and incubated for the time period indicated. Samples were subsequently washed and processed for immunofluorescence at 4°C. Identical kinetics for the off-reaction were observed when cells preincubated with gp120 and subsequently washed were incubated at 37°C with or without 100 nM soluble CD4.

Immunofluorescence. Cell-bound gp120 was determined by indirect immunofluorescence. Cells were incubated with saturating amounts of anti-gp120 mAb (anti-HIVIIIB mAb, 0.1 µg/ml; F59.1, 10 µg/ml) in 0.1 ml RPMI containing 2% FCS at 4°C for 30 min. A FITC-labeled goat anti–mouse Ab (1:100; Caltag, San Francisco, CA) was used as second-step reagent, and cell-bound fluorescence was determined using a FACS® analyzer (Becton Dickinson & Co., Mountain View, CA). Dead cells were excluded after addition of propidium iodide. Linear equivalents of mean fluorescence were obtained using the Concert 30 program (Becton Dickinson & Co.). Immunofluorescence using CD4 mAbs aimed at mapping mAb binding sites was performed similarly, except that two different nonsaturating CD4 mAb concentrations yielding between 50 and 90% of maximum fluorescence against wild type (wt)-CD4 were used. Nonsaturating concentrations were used in order to maximize sensitivity.

Calculations. The fraction of bound gp120 was determined according to the formula: $f = FL - FL_{neg}/FL_{max} - FL_{neg}$, where FL_{max} = anti-gp120 fluorescence at saturation or at the beginning ($t = 0$) of an off-rate experiment, FL = anti-gp120 fluorescence at a given gp120 concentration or at a given time point, and FL_{neg} = anti-gp120 fluorescence in the absence of gp120, respectively. We assume that $FL_{max} - FL_{neg}$ represents the concentration of CD4-gp120 complex at equilibrium and that gp120 concentrations are always in excess over the CD4 concentrations. Thus, the mass action law was transformed into $FL - FL_{neg} = [gp120_{tot} \times (FL_{max} - FL_{neg})]/(K_d + gp120_{tot})$, with $gp120_{tot}$ as the total gp120 concentration. FL_{max} and K_d were fitted using nonlinear regression of the Systat Program (Systat Inc., Evanston, IL). On-rates were determined by plotting $-\ln(1 - f)$ vs. time with slope $= (k_{off} + k_{on}) \times gp120$ (37). Results from off-rate experiments were plotted as $\ln (f)$ vs. time with slope $= -k_{off}$ (37). Slopes were determined using a linear regression program. Note that the soluble recombinant gp120 is monomeric and its binding to soluble CD4 is monovalent (data not shown). Our calculations are based on the assumption that transmembrane CD4-gp120 interaction is monovalent as well.

Graphics. For computer graphics of the CD4 structure (33), a Silicon Graphics IRIS workstation (4D/80) was used together with the Insight II program (Biosym Technologies, San Diego, CA).
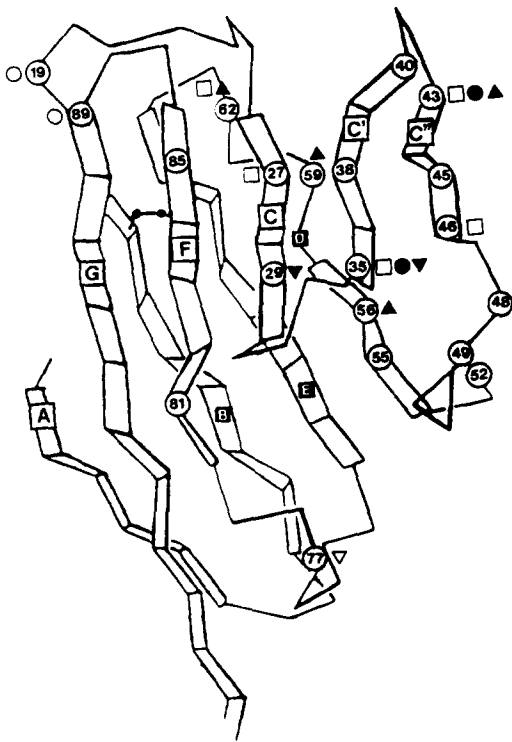
Figure 1. Location of point mutations and effects on CD4 mAb binding. Ribbon diagram representing CD4 domain 1. β strands are labeled in capital letters (front face strands, *open boxes*; back face strands, *filled boxes*) and residues analyzed herein are labeled with numbers according to their position. Residues that affect CD4 mAb binding are indicated with symbols: Leu3a (●), 19Thy5D7 (□), 18T3A9 (▲), RFT4 (▼), VIT4 (O), BL4IOT4 (▽).

Results

Generation and Expression of CD4 Mutant Molecules. 26 individual CD4 variants, substituted at 20 distinct amino acid positions, were generated by site-directed mutagenesis in order to define more precisely the key determinants of HIV gp120 binding. As shown in Fig. 1, the mutated residues include 13 amino acids located in strands C', C", and D (residues 35–62). Close to the region referred to as the C'C" ridge are residues 27 and 29, located in the C strand (Fig. 1). Amino acids 77, 81, and 85 on the F strand, and residues 19 and 89 at the top of strands B and G, respectively, lie outside the C'C" ridge (Fig. 1). Mutant CD4 cDNAs were electroporated into the murine T cell hybridoma MA5.8, and stable transfectants were characterized for surface CD4 expression. Compared with peripheral blood T lymphocytes, CD4 transfectants expressed ~10-fold less CD4 as judged by immunofluorescence (data not shown). This level of expression was comparable for individual cell lines transfected with the different CD4 mutants.

CD4 mAb Binding. To exclude the possibility that diminished HIV gp120 binding capacity was a trivial consequence of overall disruption of conformation in the first CD4 domain, each mutant was analyzed with a panel of anti-CD4 mAbs directed at the native domain 1. These anti-CD4 mAbs were selected according to published epitope mapping studies

Table 1. *Reactivity of CD4 Mutants with CD4 mAbs*

Mutation	L3a	19Thy	18T3	RFT4	VIT4	BL4	OKT4
S19Y	□□□	□□□	□□□	□□□	■■■	□□□	□□□
H27A	□□□	■■□	□□□	□□□	□□□	□□□	□□□
K35A	■■■	■■■	□□□	■■■	□□□	□□□	□□□
G38A	□□□	□□□	□□□	□□□	□□□	□□□	□□□
Q40A	□□□	□□□	□□□	□□□	□□□	□□□	□□□
F43A	□□□	■□□	■■■	□□□	□□□	□□□	□□□
F43I	■■□	■■■	■■■	□□□	□□□	□□□	□□□
F43L	□□□	□□□	□□□	□□□	□□□	□□□	□□□
F43W	□□□	□□□	■■□	□□□	□□□	□□□	□□□
F43Y	□□□	■■□	■■■	□□□	□□□	□□□	□□□
T45A	□□□	□□□	□□□	□□□	□□□	□□□	□□□
K46A	□□□	■□□	□□□	□□□	□□□	□□□	□□□
P48Q	□□□	□□□	□□□	□□□	□□□	□□□	□□□
S49V	□□□	□□□	□□□	□□□	□□□	□□□	□□□
N52A	□□□	□□□	□□□	□□□	□□□	□□□	□□□
A55V	□□□	□□□	□□□	□□□	□□□	□□□	□□□
D56A	□□□	□□□	■■□	□□□	□□□	□□□	□□□
R59A	□□□	□□□	□□□	□□□	□□□	□□□	□□□
R59K	□□□	□□□	■■□	□□□	□□□	□□□	□□□
W62Y	□□□	■■□	■■■	□□□	□□□	□□□	□□□
E77Q	□□□	□□□	□□□	□□□	□□□	■■□	□□□
T81A	□□□	□□□	□□□	□□□	□□□	□□□	□□□
E85A	□□□	□□□	□□□	□□□	□□□	□□□	□□□
E85Q	□□□	□□□	□□□	□□□	□□□	□□□	□□□
K29A/ E85A	□□□	□□□	□□□	■■■	□□□	□□□	□□□
Q89L	□□□	□□□	□□□	□□□	■■■	□□□	□□□

Binding of CD4 mAbs to cells expressing CD4 mutants was determined by immunofluorescence and compared with binding of OKT4. Reactivity was calculated as follows: {[mutant-FL(mAb) − mutant-FL(neg)]/ [mutant-FL(OKT4)−mutant-FL(neg)]}/{[wt-FL(mAb)−wt-FL(neg)]/ [wt-FL(OKT4)−wt-FL(neg)]}; where FL = linear fluorescence obtained with the specified mAb. Symbol code for reactivity is: □□□, 0.8-1; ■□□, 0.5-0.8; ■■□, 0.2-0.5; ■■■ no mAb binding.

(29, 38, 39). Leu3a, 19Thy5D7, 18T3A9, and RFT4 have been mapped to the C'C" ridge; RFT4 also to the C strand; and VIT4, and BL4IOT4 to the side of CD4 domain 1 opposite that of the C'C" ridge. mAb OKT4, which binds to a membrane proximal domain of CD4, reacted with all mutants. We used it to determine levels of CD4 expression and as a reference to compare reactivity of the other CD4 mAbs.

As shown in Table 1, each mutant had a distinct binding pattern with the panel of anti-CD4 mAbs. None of the mutants led to loss of the majority of antibody epitopes. The binding of mAbs known to interact with the C'C" ridge was reduced or eliminated by mutations in this region (e.g., at positions 35, 43, and 62), but the binding of other mAbs interacting with different parts of domain 1 was unaffected. Note that several mutations, including G38A and Q40A,

showed completely unchanged binding patterns with this set of mAbs. The restricted effect of substitutions on mAb reactivity demonstrates that these mutations exert only local effects on the structure of CD4 and suggests that the overall conformation of domain 1 is preserved. Based on these results, we interpret the effects of surface-exposed mutations to be a direct consequence of the mutated residue rather than an indirect effect of disrupting the entire domain.

These antibody binding experiments contribute additional precision to previous mapping of anti-CD4 mAbs. Substitutions that affect binding of CD4 mAbs are summarized in Fig. 1, and their positions are indicated on the model of CD4 domain 1. Leu3a, 19Thy5D7, and 18T3A9 all interact with the C'C" ridge, but their detailed pattern of sensitivity to changes in this region is different. Thus, the K35A mutant no longer binds Leu3a or 19Thy5D7, but it binds 18T3A9 with normal affinity. In contrast, 18T3A9 is more sensitive to changes at F43, D56, R59, and W62 than either of the other two mAbs. These differences probably reflect a combination of distinct footprints of antibody contact and different kinds of pockets in the antigen combining site.

Kinetics and Temperature Dependence of CD4-gp120 Interaction. We established conditions for measurement of equilibrium affinities and kinetics of gp120 interaction with wild-type and mutant CD4 molecules. As shown in Fig. 2 *A*, binding of gp120 to CD4 expressed on human T lymphocytes was slow at 4°C; a plateau was not reached even after 12 h using 10 nM gp120. The k_{on} in this experiment was 0.46 min^{-1} × μM^{-1}. Furthermore, no substantial dissociation of gp120 from CD4 was observed, even after 24 h. In contrast, association of gp120 with CD4 occurred more quickly at 37°C, and binding was complete after 2 h (Fig. 2 *B*). Moreover, gp120 almost completely dissociated from CD4 at 37°C within 2 h of incubation (Fig. 2 *B*). The temperature dependence of CD4-gp120 interaction noted here is consistent with a recent independent analysis (40). Similar kinetics for the CD4-gp120 on- and off-reactions were observed when wt-CD4 transfectants were analyzed at 37°C (Fig. 2 *C*). We note that the level of surface CD4 expression was stable after incubation with gp120. These results show that equilibrium in the CD4-gp120 interaction can be achieved by incubating for several hours at 37°C. To verify this assertion further, untreated CD4 transfectants and gp120-
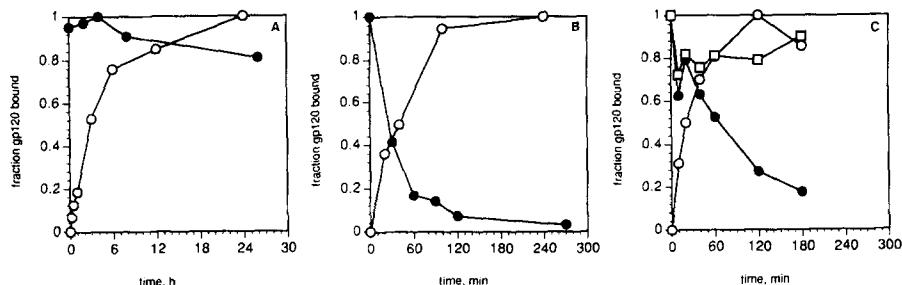
preincubated CD4 transfectants were incubated in parallel at 37°C with an intermediate concentration of gp120 (1.5 nM) for various periods of time. Subsequently, the level of cell-bound gp120 was determined. As shown in Fig. 3, similar fractions of cell-bound gp120 were observed after 1.5–4 h, regardless of whether the experiment was started with gp120-loaded or untreated cells. Equilibrium was achieved, with similar kinetics, when human CD4$^+$ T cells were analyzed (not shown). Based on these findings, we used incubation periods of 8–12 h at 37°C to determine equilibrium affinities of mutant CD4 and gp120.

Analysis of CD4 Mutants for Binding of gp120 Identifies a Key Hydrophobic Contact and Several Positively Charged Residues. The affinity of wt-CD4 and CD4 mutants for HIVIIIB gp120 was then determined. Representative equilibrium binding experiments (Fig. 4 *A*) and kinetic experiments (Fig. 4, *B* and *C*) obtained with wild-type CD4 and mutants H27A, G38A, and Q40A are shown. The summary of results obtained on all mutants is tabulated in Table 2. As shown in Fig. 4 *A*, using cells expressing wt-CD4, a K_d with a mean value of 0.9 nM was determined for HIVIIIB gp120. Mutant H27A showed a very similar binding curve (K_d = 1.6 nM); mutant G38A showed a reduced affinity (K_d = 9.4 nM); and mutant Q40A showed a slightly but significantly enhanced affinity (K_d = 0.5 nM). Experiments aimed at analyzing the on-reaction for these mutants yielded relatively similar time courses for saturation (Fig. 4 *B*). The summary of the binding rate constants listed in Table 2 demonstrates that relative to wild-type CD4, there is no change in k_{on} for H27A, a slight reduction for G38A and a two- to threefold increase for Q40A. Experiments shown in Fig.
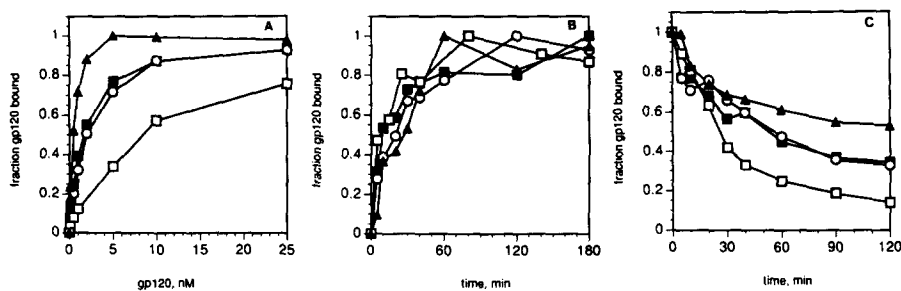
Figure 4. Determination of CD4-gp120 affinities. Equilibrium binding (A), on-rate (B), and off-rate (C) experiments performed with wt-CD4 (■) and mutants H27A (O), G38A (□), and Q40A (▲), and HIVIIIB gp120. The highest gp120 concentration in the equilibrium binding shown in A was 75 nM. Specific fluorescence of gp120 at saturation was taken as unity. Concentrations of gp120 used in on-rate experiments (B) were: wt, 3 nM; H27A, 3 nM; G38A, 15 nM; Q40A, 0.5 nM. Note that these latter experiments were performed at a concentration of gp120 estimated to be three times the K_d for each mutant as determined in the equilibrium experiments; hence, different gp120 concentrations were used in each case. Thus, the curves shown do not directly represent the association rate constant.

4 C demonstrate that the dissociation rate was almost unchanged for H27A, increased by twofold for G38A and reduced by twofold for Q40A. Note that the determinations of K_d by equilibrium and kinetic experiments are in reasonable agreement for these and other mutants.

Substitutions at positions 35, 43, and 62 had the most pronounced effects on CD4 affinity for gp120. As shown in Fig. 5 A and Table 2, mutants K35A and W62Y have dissociation constants for gp120 of 45 and 152 nM, respectively, and 500 nM gp120 was required to achieve 50% saturation when mutant F43A was utilized. 5–20-fold decreased affinities were observed for mutants K46A, P48Q, S49V, R59A, and for the double mutant K29A/E85A (Table 2). Because substitution E85A showed no effect on gp120 binding, reduced affinity of mutant K29A/E85A can probably be interpreted as an effect of replacing Lys29 with Ala. In addition to mutant Q40A, slightly enhanced affinities (K_d of 0.5 nM) were also observed for mutants T45A and R59K (Table 2). Fig. 6 illustrates the position of CD4 residues affecting HIV gp120 binding. All other mutations shown in Table 2, including substitutions at positions 77, 81, and 85, showed no effect on gp120 binding.

A Critical Role for Phe43 in HIV gp120 Binding. The above results show that F43 is the most critical of all the residues tested with regard to HIV gp120 binding. To explore further the requirements of the hydrophobic residue at this position, Phe 43 was substituted with four other hydrophobic amino acids. As shown in Fig. 5 B, substitution of Ile at position 43 resulted in a ∿500-fold loss in gp120 affinity; Trp and

Tyr substitutions gave 15–30-fold decreases; and Leu yielded only a twofold reduction. Thus, the chemical structure of the side chain at position 43 (Fig. 5 C) dramatically influences gp120 binding.

Reduced Affinities of CD4 Mutants for HIV gp120 Are Primarily Due to an Increase in k_{off}. Kinetic experiments described in Fig. 4, B and C were performed with all mutants except for F43A, F43I, and W62Y, where the low affinity would have required use of excessively high concentrations of gp120. Mutants with reduced equilibrium binding constants for gp120 showed changes predominantly in the dissociation rate constants (Table 2). For example, the k_{off} for K35A was 173 min^{-1} × 10^{-3} compared with 12.5 min^{-1} × 10^{-3} for wt-CD4. In some cases, however, such as mutants K35A, F43Y, K46A, and R59A, a decreased association rate was also observed when compared to wt-CD4. It should be mentioned that like wt-CD4, none of the mutants showed any dissociation of bound gp120 at 4°C within a period of 2 h. Kinetics of mutants F43A, F43I, and W62Y were not analyzed at 37°C due to their low affinity. Nevertheless, dissociation of bound gp120 studied at 25°C showed off-rates in the order F43A > F43I > W62Y > wt (not shown). Q40A showed the most marked increase in k_{on} (16.5 min^{-1} vs. 6.1 min^{-1} × μM^{-1} for wt-CD4).

Mutations in CD4 Affect Binding of gp120 from More than One HIV Stain. To determine whether or not the same residues in CD4 influence the binding of diverse HIV strains, CD4 mutants with reduced affinities for HIVIIIB gp120 were tested in equilibrium binding experiments for their ability
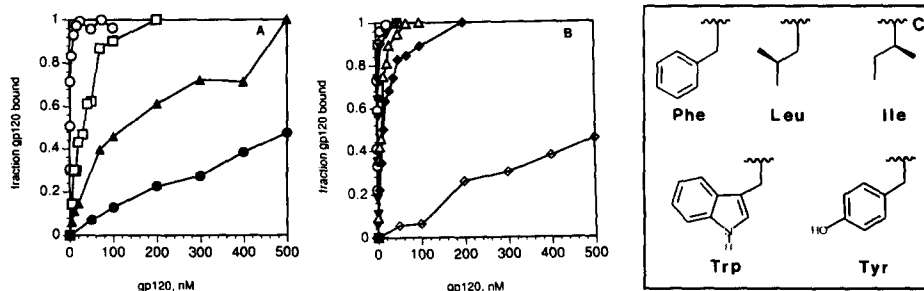

Figure 5. Affinity of CD4 mutants for HIVIIIB gp120. Equilibrium binding experiments with wt-CD4 (O) and mutants K35A (□), F43A (●), W62Y (▲), F43L (▼), F43W (△), F43Y (◆), and F43I (◇). The highest gp120 concentration in this experiment was 500 nM. Fluorescence of gp120 at saturation was extrapolated for mutants F43A and F43I according to their level of CD4 expression and the ratio of CD4- vs. gp120-specific fluorescence as obtained for wt and other mutants at saturation.

Table 2. *Affinity of CD4 Mutants for HIVIIIB gp120*

Mutation	Kinetic experiments			Equilibrium conditions (K_d)
	k_{on}	k_{off}	k_{off}/k_{on}	
	$min^{-1} \times \mu M^{-1}$	$min^{-1} \times 10^{-3}$	nM	nM
wt	6.1 ± 2.4	12.5 ± 1.2	2.0	0.9 ± 0.3
S19Y	5.9	13.1	2.2	1.2
H27A	5.5	13.3	2.4	1.6
K35A	1.8	173.3	98	45
G38A	3.2	27.7	8.7	9.4
Q40A	16.5	5.8	0.4	0.5
F43A	ND	ND	ND	500
F43I	ND	ND	ND	500
F43L	5.9	21.6	3.7	2.5
F43W	3.9	76.9	20	16
F43Y	1.7	53.3	32	32
T45A	7.7	9.6	1.3	0.6
K46A	2.0	33.0	16	19
P48Q	4.5	34.6	7.6	4.5
S49V	3.6	46.2	13	13
N52A	5.7	10.2	1.8	0.8
A55V	5.0	18.2	3.6	2.4
D56A	4.3	12.2	2.9	1.6
R59A	2.4	26.6	11	7.9
R59K	7.1	9.5	1.3	0.6
W62Y	ND	ND	ND	152
E77Q	8.9	11.6	1.3	1.3
T81A	3.5	18.2	5.2	1.5
E85A	7.2	16.9	2.4	1.3
E85Q	3.6	16.9	4.7	1.5
K29A/E85A	3.7	49.5	13	6.7
Q89L	7.3	12.8	1.8	1.2

to bind gp120 derived from the structurally distinct HIV strain SF2. The affinity of wt-CD4 for SF2 gp120 is more than one order of magnitude lower than for HIVIIIB gp120 (K_d = 20 vs. 0.9 nM). As shown in Table 3, all mutations with reduced affinities for HIVIIIB gp120 showed diminished affinities also for SF2 gp120. Moreover, for each individual mutant the change in affinity for SF2 gp120 was comparable to the change observed with HIVIIIB gp120 (Table 3).

Discussion

We have established experimental conditions for measuring the affinity of gp120 and mutant CD4 at equilibrium, as well as for determining the rate constants for association and dissociation. The kinetics are strongly temperature dependent. The rate of dissociation is negligible at 4°C, and it was there-fore necessary to perform the studies at 37°C in order to achieve equilibrium. CD4 is not rapidly endocytosed when expressed on the surface of lymphoid cells (41), and we could determine gp120 binding curves over an 8-12-h period in stable murine T cell line transfectants. Most previous experiments on gp120 binding to expressed mutants of CD4 were performed at lower temperature (12, 28, 30–32), and they were therefore primarily measurements of relative on-rates rather than of equilibrium affinities. The properties of the K35A mutant are a useful illustration: the effect of the change on the rate of CD4-gp120 association is much smaller than its effect on dissociation. A measurement sensitive only to k_{on} would have shown a small change in apparent binding. In other cases, there are changes in both association and dissociation rate constants, but only the equilibrium binding measurements, which take both into account, reveal the full effect of the substitution.

Table 3. *Mutant Reactivity with SF2 gp120*

Mutant	K_d for SF2 gp120	Fold decrease of affinity for SF2 gp120	Fold decrease of affinity for HIVIIIB gp120
	nM		
wt	20	1	1
K35A	1,000	50	50
G38A	120	6	10
F43A	nsb	ND	550
F43W	400	20	18
K46A	350	17	21
P48Q	140	7	5
S49V	200	10	14
R59A	200	10	9
W62Y	>1,000	>50	169
K29A/E85A	200	10	7

Affinities for SF2 gp120 were determined using equilibrium binding conditions. nsb, no specific binding.

The most striking effects uncovered here are those associated with substitution at Phe43. The exposed hydrophobic side chain (Fig. 6) is an unusual feature of CD4, and additional studies from our laboratory suggest that it is important for the normal function of CD4 in binding to class II MHC molecules (Moebius et al., manuscript submitted for publication). We observe a graded series of changes when other hydrophobic side chains are introduced at this position. Substituting tyrosine or tryptophan introduces a polar atom and increases side chain volume, leading to 30-fold and 15-fold decreases in affinity, respectively, but complete removal of the aromatic group in the F43A mutant leads to an even more pronounced effect (>500-fold). A leucine at position 43 produces a very modestly reduced affinity, but isoleucine is as unfavorable as alanine. Not only must the residue at 43 have a pronounced hydrophobic character, it must also have a particular shape. The simplest explanation is that a pocket on gp120 normally accommodates Phe43 and that this pocket can admit a leucine side chain but not a β-branched isoleucine. Several mAbs, including Leu3a, have the same strong preference (Table 1).

Removal of any of four positively charged side chains (K29, K35, K46, and R59) in the vicinity of F43 also reduces affinity for gp120 (Fig. 6). The strongest effect (50-fold) is obtained with mutant K35A. Preserving the charge at position 59 in CD4 by replacing arginine with lysine actually increases affinity for gp120 by a small amount. The distances between the positive charges and the $C\beta$ of Phe43 are 9.35, 9.81, 11.32, and 19.57 Å for R59, K35, K46, and K29, respectively. The importance of K35 has not been noticed in most previous mutagenesis studies, perhaps because its influence is largely on the rate of dissociation. Recent experiments with human/rat CD4 chimeras show that in order to be a functional

receptor, the molecule must have a human sequence at K35 (where rat CD4 has threonine), consistent with our results (42).

Substituting alanine for glutamine at position 40 or for threonine at position 45 results in a small enhancement of gp120 binding. Both these side chains lie on the molecular surface close to Phe43 (Fig. 6), and it is plausible to suppose that they interfere slightly with the correct fit of gp120 to CD4. The added methyl group in the G38A variant also appears to interfere, leading to a 5–10-fold decrease in affinity for gp120. We conclude that surface topography in the neighborhood of Phe43, including the entire C'C" turn from residue 38 to 45, can influence the gp120 interaction.

This conclusion is reinforced by the even more substantial effect of the W62Y substitution. Most of the tryptophanyl side chain is buried beneath the C'C" turn, and its bulk is probably critical for the way the turn projects from the edge of the CD4 molecule (Fig. 6). We chose tyrosine as a substitution in order to preserve the hydrophobic character of this residue and to maintain a hydrogen-bonding function. Nonetheless, the modest reduction in side chain volume and the slight repositioning of a hydrogen-bonding group (the phenolic hydroxyl of tyrosine lies ~2 Å farther from $C\beta$ than does the indole nitrogen of tryptophan) leads to a 150-fold loss of affinity.

The properties of several of our mutants also demonstrate that the gp120 interaction is sensitive to the conformation of the "lower" part of the C" ridge (the C" D corner). P48Q and S49V both have somewhat reduced affinity for gp120. Proline 48 lies at the edge of this CD4 molecule, at the end of the C" strand, and serine 49 points into the C" D corner (Fig. 6). Its side chain hydroxyl is hydrogen bonded to a buried water. The valine substitution may alter the shape of the C" D corner by eliminating a hydrogen-bonding function. The slightly lower affinity of A55V, which points into the C" D corner from the opposite face of domain 1, may also be due to a local distortion in this part of the molecule.

The results and conclusions summarized here are largely consistent with previous binding studies, which demonstrate an effect on the gp120 interaction from substitutions at residue 29, 40, 43, 46, 48, 49, 59, or 62 (31, 32, 43, 44). Likewise, the lack of effect from a substitution at 19, 27, 56, or 89 is consistent with the literature (31, 32, 43, 44). In contrast, we do not observe any change in affinity resulting from mutation of 52, 77, 81, or 85, all of which were reported to influence gp120 binding (32). The basis of the disparity is unclear, but a third study also reports no effects from substitutions at 81 and 85 (44). Our findings that mutations at these charged (E77 and E85) and polar (S19, T81, and Q89) residues show unaffected gp120 affinity do not support the notion that residues spatially well removed from the C'C" ridge contribute critically to the gp120 interaction. Residues near the C'C" ridge that are not included in this study have been examined qualitatively in other's work. Alterations of surface residues N30, S31, N32, Q33, K50, D53, R58, or S60 have no effect on gp120 binding (31, 32). Changing buried residue I36, L37, L51, R54, or S57 produces an overall
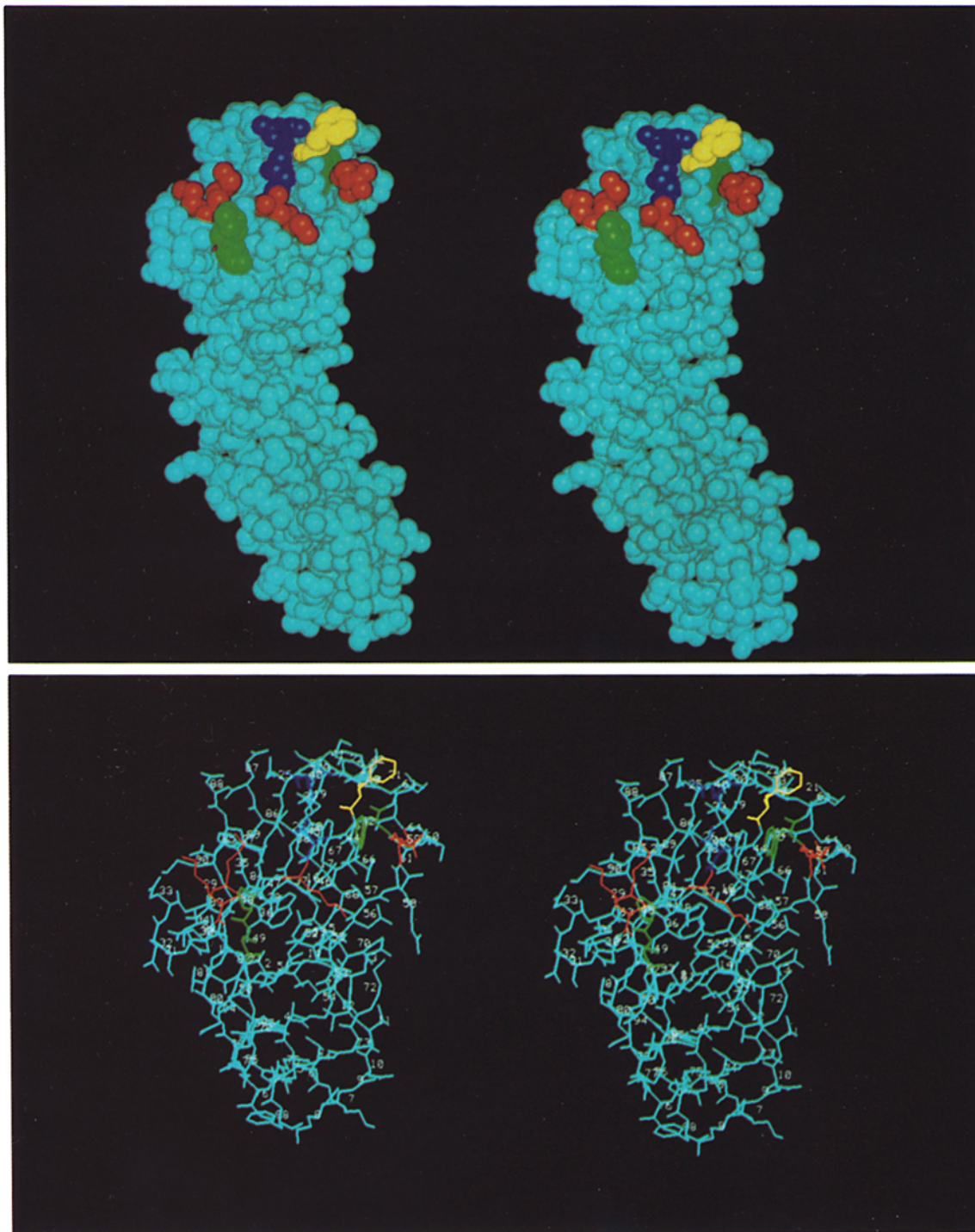
Figure 6. Illustration of the gp120 binding site. Stereo views of (*A*) space-filling model of CD4 domains 1 and 2, and (*B*) α-carbon trace model of CD4 domain 1 according to the atomic structure of CD4 (33). Charged residues involved in gp120 binding are shown in red (K29, K35, K46, and R59). The hydrophobic residue (F43) involved in gp120 binding is shown in yellow. The buried residue that affects gp120 binding by altering the C′C″ ridge (W62) and the buried (S49) and exposed (P48) residues altering the C″D turn are shown in green. Amino acids (Q40 and T45) whose mutation to alanine enhanced gp120 binding are shown in dark blue.

loss of conformational stability in domain 1, as deduced from the effect of reactivity with a varity of CD4 mAbs (32). Mutations at G41, L44, and G47 are reported to decrease affinity for gp120 (31, 32), and examination of the model shows that the changes in question would be expected to perturb the conformation of the C′C″ turn or the C″D corner. For example, leucine 44 packs against tryptophan 62 and helps determine the projecting conformation of phenylalanine 43. The

Q40P and T45P mutations, reported to interfere with gp120 binding (43), would also be expected to alter the C'C" turn.

We conclude that the principal determinant of gp120 binding is a continuous region on the surface of domain 1 covering ~900 Å² of accessible surface. This site contains Phe43 near its center partially surrounded by positively charged residues Lys29, Lys35, Lys46, and Arg59. The importance of positively charged residues in the vicinity of Phe43 is interesting in view of a previous report where three negatively charged residues in gp120 have been demonstrated to be critical for binding to CD4 (45). Two of the three residues are conserved not only among HIV-1 isolates, but also in HIV-2 and in SIV strains. The contact between the viral glycoprotein and its receptor might therefore include a set of ionic interactions flanking a central hydrophobic patch.

The binding site on CD4 for its normal interaction with class II MHC molecules is more complex than the site for gp120 (12, 43, 46). It includes several other parts of the molecular surface in domains 1 and 2, in addition to the C'C" ridge. It is striking, however, that when the same CD4 mutations analyzed here were examined for their capacity to bind class II MHC molecules, similar effects were observed (Moebius et al., manuscript submitted for publication). In particular, the alterations that reduce gp120 binding (K35A, F43A, K46A, S49V, R59A, and W62Y) also diminish rosette formation between CD4-transfected COS-1 cells and class II MHC-expressing B cells. A surface region with a projecting hydrophobic side chain (Phe43) and adjacent positively charged residues thus also appears to be important for the class II MHC interaction. The overlap of HIV gp120 and class II binding sites requires that development of receptor-based HIV inhibitors avoids drugs with immunosuppressive properties. Our detailed analysis of the contribution of residues in CD4 domain 1 to HIV gp120 binding gives a quantitative assessment of key components in the virus binding site, with such developments in mind.

Address correspondence to Ulrich Moebius, Laboratory of Immunobiology, Dana Farber Cancer Institute, 44 Binney Street, Boston, MA 02115.

References

1. Reinherz, E.L., P.C. Kung, G. Goldstein, R.H. Levey, and S.F. Schlossman. 1980. Discrete stages of intrathymic differentiation: Analysis of normal thymocytes and leukemic lymphoblasts of T lineage. *Proc. Natl. Acad. Sci. USA.* 77:1588.

2. Kruisbeek, A.M., J.J. Mong, B.J. Fowlkes, J.A. Carmen, S. Bridges, and D.L. Longo. 1985. Absence of the Lyt-2⁻,L3T4⁺ lineage of T cells in mice treated neonatally with anti-I-A correlates with absence of intrathymic I-A-bearing antigen-presenting cell function. *J. Exp. Med.* 161:1029.

3. Ramsdell, F., and B.J. Fowlkes. 1989. Engagement of CD4 and CD8 accessory molecules is required for T cell maturation. *J. Immunol.* 143:1467.

4. Engleman, E.G., C.J. Benike, C. Grumet, and R.L. Evans. 1981. Activation of human T lymphocyte subsets: helper and suppressor/cytotoxic T cells recognize and respond to distinct histocompatibility antigens. *J. Immunol.* 127:2124.

5. Biddison, W.E., P.E. Rao, M.A. Talle, G. Goldstein, and S. Shaw. 1982. Possible involvement of the OKT4 molecule in T cell recognition of class II HLA antigens: evidence from studies of cytotoxic T lymphocytes specific for SB antigens. *J. Exp. Med.* 156:1065.

6. Krensky, A.M., C.S. Reiss, J.W. Mier, J.L. Strominger, and S.J. Burakoff. 1982. Long-term human cytolytic T cell lines allospecific for HLA-DR6 antigen are OKT4+. *Proc. Natl. Acad. Sci. USA.* 79:2365.

7. Meuer, S.C., S.F. Schlossman, and E.L. Reinherz. 1982. Clonal analysis of human cytotoxic T lymphocytes: T4⁺ and T8⁺ effector T cells recognize products of different major histocompatibility complex regions. *Proc. Natl. Acad. Sci. USA.* 79:4395.

8. Eichmann, K., J.-I. Jönsson, I. Falk, and F. Emmrich. 1987. Effective activation of resting mouse T lymphocytes by cross-linking submitogenic concentrations of the T cell antigen receptor with either Lyt-2 or L3T4. *Eur. J. Immunol.* 17:643.

9. Owens, T., D.S.B. Fazekas, and J.F.A.P. Miller. 1987. Coaggregation of the T-cell receptor with CD4 and other T-cell surface molecules enhances T-cell activation. *Proc. Natl. Acad. Sci. USA.* 84:9209.

10. Meuer, S.C., R.E. Hussey, J.C. Hodgdon, T. Hercend, S.F. Schlossman, and E.L. Reinherz. 1982. Surface structures involved in target recognition by human cytotoxic T lymphocytes. *Science (Wash. DC).* 218:471.

11. Doyle, C., and J.L. Strominger. 1987. Interaction between CD4

and class II MHC molecules mediates cell adhesion. *Nature (Lond.).* 330:256.

12. Clayton, L.K., M. Sieh, D.A. Pious, and E.L. Reinherz. 1989. Identification of human CD4 residues affecting class II MHC versus HIV-1 gp120 binding. *Nature (Lond.).* 339:548.

13. Reinherz, E.L., P.C. Kung, G. Goldstein, and S.F. Schlossman. 1979. A separation of functional subset of human T cells by a monoclonal antibody. *Proc. Natl. Acad. Sci. USA.* 76:4061.

14. Reinherz, E.L., P.C. Kung, G. Goldstein, and S.F. Schlossman. 1979. Further characterization of the human inducer T cell subset defined by monoclonal antibody. *J. Immunol.* 234:2894.

15. Dalgleish, A.G., P.C.L. Beverley, P.R. Clapham, D.H. Crawford, M.F. Greaves, and R.A. Weiss. 1984. The CD4 (T4) antigen is an essential component of the receptor for the AIDS retrovirus. *Nature (Lond.).* 312:763.

16. Klatzmann, D., E. Champagne, S. Chamaret, J. Gruest, D. Guetard, T., Hercend, J.-C. Gluckman, and L. Montagnier. 1984. T lymphocyte T4 molecule behaves as the receptor for human retrovirus LAV. *Nature (Lond.).* 312:767.

17. McDougal, J.S., A. Mawle, S.P. Cort, J.K.A. Nicholson, G.D. Cross, J.A. Schepper-Campbell, D. Hicks, and J. Sligh. 1985. Cellular tropism of the human retrovirus HTLV/LAV. I. Role of T cell activation and expression of the T4 antigen. *J. Immunol.* 135:3151.

18. Maddon, P.J., A.G. Dalgleish, J.S. McDougal, P.R. Clapham, R.A. Weiss, and R. Axel. 1986. The T4 gene encodes the AIDS virus receptor and is expressed in the immune system and the brain. *Cell.* 47:333.

19. Stein, B.S., S.D. Gouda, J.D. Lifson, R.C. Penhallow, K.G. Bensch, and E.G. Engleman. 1987. pH-independent HIV entry into CD4-positive T cells via virus envelope fusion to the plasma membrane. *Cell.* 49:659.

20. McDougal, J., M. Kennedy, J. Sligh, S. Cort, A. Mawle, and J. Nicholson. 1986. Binding of the HTL VIII/LAV to T4⁺ T cells by a complex of the 110k viral protein and the T4 molecule. *Science (Wash. DC).* 231:382.

21. Lane, M.C., J.L. Depper, W.C. Green, G. Whalen, T Waldmann, and A.S. Fauci. 1985. Qualitative analysis of immune function in patients with the acquired immunodeficiency syndrome. *N. Engl. J. Med.* 313:79.

22. Lyerly, H.K., T.J. Matthews, A. Langlois, D. Bolognesi, and K. Weinhold. 1987. Human lymphotropic virus IIIb glycoprotein (gp120) bound to CD4 determinants on normal lymphoctyes and expressed by infected cells serves as target for immune attack. *Proc. Natl. Acad. Sci. USA.* 84:4601.

23. Sodroski, J., W. Goh, C. Rosen, K. Campbell, and W. Haseltine. 1986. Role of the HTLVIII/LAV envelope in syncitia formation and cytopathicity. *Nature (Lond.).* 322:470.

24. Siliciano, R., T. Lawton, C. Knall, P. Berman, T Gregory, and E. Reinherz. 1988. Analysis of host-virus interactions in AIDS with anti-gp120 T cell clones: effect of HIV sequence variation and a mechanism for CD4+ T cell depletion. *Cell.* 54:561.

25. Shalaby, M.R., J.F. Krowka, T.J. Gregory, S. Hirabayashi, S. McCabe, D. Kaufman, D. Stites, and A. Ammann. 1987. The effects of human immunodeficiency virus recombinant envelope protein on immune cell functions in vitro. *Cell. Immunol.* 110:140.

26. Maddon, P.J., D.R. Littman, M. Godfrey, D.E. Maddon, L. Chess, and R. Axel. 1985. The isolation and nucleotide sequence of a cDNA encoding the lymphocyte protein T4: a new member of the immunoglobulin family. *Cell.* 42:93.

27. Richardson, N.E., N.R. Brown, R.E. Hussey, A. Vaid, T.J. Matthews, D.P. Bolognesi, and E.L. Reinherz. 1988. Binding site for human immunodeficiency virus coat protein gp120 is located in the NH₂-terminal region of T4 (CD4) and requires the intact variable-region-like domain. *Proc. Natl. Acad. Sci. USA.* 85:6102.

28. Arthos, J., K.C. Deen, M.A. Chaikin, J.A. Fornwald, G. Sathe, Q.J. Sattentau, P.R. Clapham, R.A. Weiss, J.S. McDougal, C. Pietropaolo, R. Axel, A. Truneh, P.J. Maddon, and R.W. Sweet. 1989. Identification of the residues in human CD4 critical for the binding of HIV. *Cell.* 57:469.

29. Peterson, A., and B. Seed. 1988. Genetic analysis of monoclonal antibody and HIV binding sites on the human lymphocyte antigen CD4. *Cell.* 54:65.

30. Mizukami, T., T.R. Fuerst, E.A. Berger, and B. Moss. 1988. Binding region for human immunodeficiency virus (HIV) and epitopes for HIV-blocking monoclonal antibodies of the CD4 molecule defined by site-directed mutagenesis. *Proc. Natl. Acad. Sci. USA.* 85:9273.

31. Brodsky, M.H., M. Warton, R.M. Myers, and D.R. Littman. 1990. Analysis of the site in CD4 that binds to the HIV envelope glycoprotein. *J. Immunol.* 144:3078.

32. Ashkenazi, A., L.G. Presta, S.C. Marsters, T.R. Camerato, K.A. Rosenthal, B.M. Fendly, and D.J. Capon. 1990. Mapping the CD4 binding site for human immunodeficiency virus by alanine-scanning mutagenesis. *Proc. Natl. Acad. Sci. USA.* 87:7150.

33. Wang, J., Y. Yan, T.P.J. Garrett, J. Liu, D.W. Rodgers, R.L. Garlick, G.E. Tarr, Y. Husain, E.L. Reinherz, and S.C. Harrison. 1990. Atomic structure of a fragment of human CD4 containing two immunoglobulin-like domains. *Nature (Lond.).* 348:411.

34. Ryu, S.-E., P.D. Kwong, A. Truneh, T.G. Porter, J. Arthos, M. Rosenberg, X. Dai, N.-H. Xuong, R. Axel, R.W. Sweet, and W.A. Hendrickson. 1990. Crystal structure of an HIV-binding recombinant fragment of human CD4. *Nature (Lond.).* 348:419.

35. Clayton, L.K., R.E. Hussey, R. Steinbrich, H. Ramachandran, Y. Husain, and E.L. Reinherz. 1988. Substitution of murine for human CD4 residues identifies amino acids critical for HIV gp120 binding. *Nature (Lond.).* 335:363.

36. Ohashi, O.S., T.W. Mak, P. van den Elsen, Y. Yanagi, Y. Yoshikai, A.F. Calman, C. Terhorst, J.D. Stobo, and A. Weiss. 1985. Reconstitution of an active surface T3/T-cell antigen receptor by DNA transfer. *Nature (Lond.).* 316:606.

37. Munck, A. 1976. General aspects of steroid hormone-receptor interactions. *In* Receptors and Mechanism of Action of Steroid Hormones, Part I. J.R. Pasqualini, editor. Marcel Dekker, Inc., New York. 1–40.

38. Sattentau, Q.J., J. Arthos, K. Deen, N. Hanna, D. Healey, P.C.L. Beverley, R. Sweet, and A. Truneh. 1989. Structural analysis of the human immunodeficiency virus-binding domain of CD4. *J. Exp. Med.* 170:1319.

39. Healey, D.G., L. Dianda, D. Buck, K. Schroeder, A. Truneh, Q.J. Sattentau, and P.C.L. Beverley. 1991. A highly selected panel of anti-CD4 antibodies fails to induce anti-idiotypic antisera mediating human immunodeficiency virus neutralization. *Eur. J. Immunol.* 21:1491.

40. Dimitrov, D.S., K. Hillman, J. Manischewitz, R. Blumenthal, and H. Golding. 1992. Kinetics of soluble CD4 binding to cells expressing human immunodeficiency virus type 1 envelope glycoprotein. *J. Virol.* 66:132.

41. Pelchen-Matthews, A., J.E. Armes, G. Griffiths, and M. Marsh. 1991. Differential endocytosis of CD4 in lymphocytic cells. *J. Exp. Med.* 173:575.

42. Schockmel, G.A., C. Somoza, S.J. Davis, A.F. Williams, and D. Healey. 1992. Construction of a binding site for human immunodeficiency virus type I gp120 in rat CD4. *J. Exp. Med.* 175:301.

43. Fleury, S., D. Lamarre, S. Meloche, S.-E. Ryu, C. Cantin, W.A. Hendrickson, and R.-P. Sekaly. 1991. Mutational analysis of the interaction between CD4 and class II MHC: class II antigens contact CD4 on a surface opposite the gp120 binding site. *Cell.* 66:1037.

44. Choe, H.-R., and J. Sodroski. 1992. Contribution of charged amino acids in the CDR2 region of CD4 to HIV-1 gp120 binding. *J. Acquired Immune Defic. Syndr.* 5:204.

45. Olshevsky, U., E. Helseth, C. Furman, J. Li, W. Haseltine, and J. Sodroski. 1990. Identification of individual human immunodeficiency virus type 1 gp120 amino acids important for CD4 receptor binding. *J. Virol.* 64:5701.

46. Lamarre, D., A. Ashkenazi, S. Fleury, D.H. Smith, R.-P. Sekaly, and D.J. Capon. 1989. The MHC-binding and gp120-binding functions of CD4 are separable. *Science (Wash. DC).* 245:743.